

## Next-Generation Sequencing of Endobronchial Ultrasound Transbronchial Needle Aspiration Specimens in Lung Cancer

To the Editor:

Endobronchial ultrasound transbronchial needle aspiration (EBUS-TBNA) is widely used to diagnose lung cancer, providing diagnostic material in high-prevalence cohorts in more than 90% of patients, including lymph node material for genetic analysis (1–4). Rapid multiplex genetic analysis of such material by next-generation sequencing (NGS) shows great promise as a means to identify mutations in cell signaling pathways that can be targeted by drugs approved by the U.S. Food and Drug Administration (FDA), perhaps after their repurposing. This ability to reveal novel therapeutic options by analysis of formalin-fixed paraffin-embedded (FFPE) cell block material is well matched to EBUS-TBNA samples, where there can be abundant material in patients with either localized or metastatic lung cancer. The primary purpose of this NGS study was to apply the 48-gene TruSeq Amplicon Cancer Panel (TSCAP; Illumina, San Diego, CA) (5) to FFPE specimens derived from EBUS-TBNA to determine whether mutations in common actionable genes might be readily detected. The study cohort was not preselected, and EBUS-TBNA procedures were as per our usual practice, with either moderate sedation or general anesthesia, using laryngeal mask airway. The study protocol was approved by the Royal Brisbane and Women's Hospital and The University of Queensland Institutional Ethical Review boards (HREC/12/QRBW/445 and UQ-HREC2016000027). Some of the results of this study have been previously reported in the form of an abstract (6).

A total of 76 consecutive patients with a provisional diagnosis of lung cancer were recruited prospectively on referral for EBUS-TBNA diagnosis of mediastinal or hilar nodes. Olympus 21G needles (NA-201SX-4021; Olympus Australia, Melbourne, Australia) were used with suction applied and 8–10 agitations per pass. Malignancy was confirmed in 66 cases (42 adenocarcinoma, 11 small cell lung cancer, 10 squamous cell carcinoma, and 3 metastatic malignancy: renal cell carcinoma, melanoma, mesothelioma); the remaining 10 were ultimately diagnosed as benign disease and excluded from further study. The 66 malignant cases had a median age of 67 years, ranging from 29 to 89 years, and a male:female ratio of 0.56. For the primary lung cancers,

10 cases had N1 disease, and 53 cases (84%) had N2 or N3 disease; 26 cases (41%) had distant metastases at the time of procedure. A median of 3 needle passes were made (range, 2–5), and a positive diagnosis of malignancy was made by rapid onsite evaluation in 64 procedures (97%). Subsequent cytopathology found that all adenocarcinomas were ALK-immunohistochemistry-negative, and routine diagnostic *EGFR* sequencing (competitive allele-specific TaqMan PCR [castPCR; Life Technologies, Carlsbad, CA]) identified 2 cases (of 38 tested) with somatic mutations in *EGFR* (one exon 19 deletion and one exon 21 c.2573T>G [Leu858Arg] mutation).

Genomic DNA was extracted from ten to twenty 7- $\mu$ m sections of FFPE cell-block material with variable results: median DNA yield 88 ng (range, 0–4,800 ng). More needle passes did not necessarily yield more DNA. For example, the median DNA yield for three needle passes was 120 ng (range, 1–2,500 ng) compared with 94 ng (range, 5–2,600 ng) for four needle passes and 26 ng (range, 4–1665 ng) for five needle passes (Kruskal-Wallis test,  $P = 0.7902$ ). A semiquantitative grading of tumor cell abundance in the cell block was developed, assessing tumor cell density (sparse, moderate, or dense) and appearance (single cells, clumps of <5, 5–10, or >10 cells). As expected, a higher tumor cell abundance was associated with a higher DNA yield (Kruskal-Wallis test,  $P = 0.0030$ ).

Sufficient genomic DNA for amplicon library preparation ( $\geq 50$  ng) was obtained from FFPE material for 40/66 patients (median DNA input amount: 185 ng; range, 47–395 ng). Libraries were prepared with the TruSeq Amplicon Cancer Panel and sequenced on a MiSeq (Illumina), with the sequence coverage of targeted bases ranging from  $133\times$  to  $1,253\times$  (median,  $513\times$ ). A total of 46 potential somatic variants were identified in 29 tumor samples, which included 12 silent, 31 missense, and 3 nonsense alterations across 21 genes (Figure 1). Twenty-four of the samples contained at least one nonsilent, likely somatic mutation (range, one to three mutations). The most common was *TP53*; other well-described alterations included activating codon 12 and codon 61 mutations in *KRAS*, as well as mutations in *RB1*, *PIK3CA*, *PTEN*, and *EGFR*. These changes are similar to mutations detected from resected lung specimens in other studies (7). NGS confirmed the exon 21 c.2573T>G (Leu858Arg) *EGFR* mutation detected by routine diagnostic sequencing. The second known *EGFR* mutation (exon 19 deletion) that was identified by diagnostic *EGFR* sequencing in our cohort was not tested, as there was insufficient DNA for amplicon library preparation.

A number of the nonsilent, putative somatic mutations affected genes involved with intracellular signaling pathways that may become actionable targets for FDA-approved drugs (8). This gene list is *KRAS*, *EGFR*, *ALK*, *KIT*, *MET*, *FLT3*, *CSF1R*, *PTEN*, *PIK3CA*, and *AKT*. Mutations in *KRAS* have the potential to drive tumor growth via MEK/ERK signaling pathway activation that can be targeted by Selumetinib (AZD6244, ARRY-142886; AstraZeneca, Cambridge, UK). Mutations in tyrosine kinase receptor genes (*EGFR*, *ALK*, *KIT*, *MET*, *FLT3*, and *CSF1R*) can potentially be targeted by receptor tyrosine kinase inhibitors such as erlotinib (Tarceva; Astellas Pharma Inc., Tokyo, Japan), afatinib (Gilotrif; Boehringer Ingelheim Pharmaceuticals, Inc., Ridgefield, CT), and gefitinib (Iressa; AstraZeneca), which are approved by the FDA for first-line treatment of metastatic non-small-cell lung cancer tumors bearing *EGFR* exon 19 deletions or

Supported by a Pathology Queensland Study Education and Research grant, a Queensland Institute of Medical Research Berghofer Keith Boden fellowship (K.N.), and the National Health and Medical Research Council of Australia (NHMRC CDF2; 1112113) (N.W.).

Author Contributions: D.F. conceived the study, managed patient consent, performed endobronchial ultrasound transbronchial needle aspiration (EBUS-TBNA), and analyzed data; F.B. managed patient consent and performed EBUS-TBNA; M.S. and L.N. contributed to study design, performed onsite pathology review of EBUS-TBNA, performed pathology and clinical annotation of cases, and interpreted the data; A.E.M.R. performed digital scanning; A.E.M.R., D.B., A.J.D., and P.T.S. performed DNA extractions and sequencing and analyzed data; S.K., K.N., J.P., and N.W. analyzed sequencing data; S.R.L., P.T.S., and N.W. contributed to study design and interpretation of findings. All authors contributed to drafting the manuscript and approved the final version.

# CORRESPONDENCE

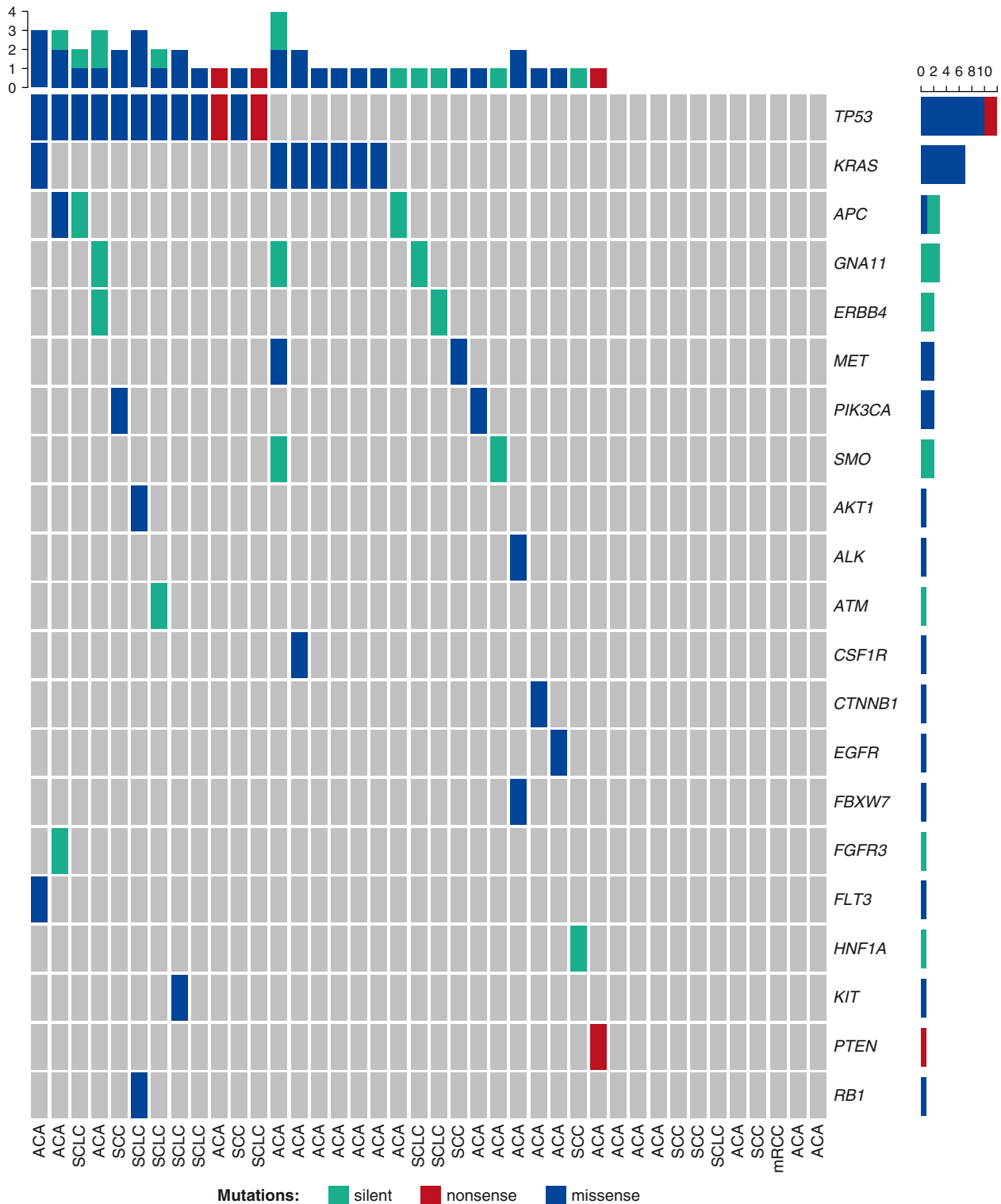


**Figure 1.** Silent and nonsilent variants detected by targeted amplicon sequencing of 40 patient endobronchial ultrasound transbronchial needle aspiration lymph node samples using the TruSeq Amplicon Cancer Panel (Illumina). Diagnosis annotations: adenocarcinoma (ACA), squamous cell carcinoma (SCC), small cell carcinoma (SCLC), metastatic renal cell carcinoma (mRCC). Reported mutations had >200 reads at the variant position, >10% variant allele frequency, <1% general population allele frequency, and passed manual review using Integrative Genomics Viewer. The 46 mutations include 39 (85%) discrete mutations, of which 24 (62%) were documented in the Catalogue of Somatic Mutations in Cancer (COSMIC v75). Single-nucleotide polymorphisms were called using qSNP, annotated using Ensemble v75 and dbSNP (v 141), and effect prediction estimated using SnpEff 4.0e (build 2014-09-13). Prepared in R version 1.10.2, using ComplexHeatmap, Zuguang Gu (2016).

exon 21 c.2573T>G (Leu858Arg) substitutions. Midostaurin (PKC412; Novartis Pharmaceuticals, Basel, Switzerland), dovitinib (TKI-258, CHIR-258; Novartis Pharmaceuticals), and cabozantinib (Cometriq; Exelixis, Inc., San Francisco, CA) have broad tyrosine kinase inhibitor activity, and the combination of cabozantinib with erlotinib has undergone a phase 2 trial for *EGFR* mutation–negative non–small-cell lung cancer with favorable results (NCT01708954) (9). Mutations within *PTEN*, *PIK3CA*, and *AKT* can disrupt the mammalian target of rapamycin (mTOR) pathway that regulates cell metabolism and proliferation. New-generation mTOR signaling suppressors are under development but are not approved by the FDA (10).

This study has successfully demonstrated the application of amplicon sequencing to the detection of potentially actionable mutations in diagnostic EBUS-TBNA samples. This was achieved without increasing the overall number of needle passes beyond current literature (11). Approximately two-thirds of EBUS-TBNA lymph node samples provided adequate DNA for NGS, which revealed a number of known driver or putatively activating mutations. Importantly, we found that a higher tumor cell abundance in the biopsied material, rather than a higher number of needle passes, translated into better sequencing hit rate. As is observed in routine EBUS-TBNA practice, some malignant nodes are very highly cellular, whereas others have more stroma and vessels interspersed; the former could reasonably expect to have high DNA content even with two passes, whereas the latter might take three or four passes to obtain sufficient DNA.

This approach therefore holds great promise for application to clinical lung cancer specimens. It is important to note that our samples were from cases with a very high pretest likelihood of cancer and a high prevalence of malignancy in the sampled nodes. Such patients are often appropriate recipients for genetically tailored therapies. Conversely, populations with less advanced disease, such as presurgical staging patients, are likely to have significantly lower prevalence of malignant cells, and consequently yield a lower relative abundance of tumor DNA. Where nodes are sampled with lower likelihood of cancer (as in staging procedures [3]), it may be that other ways to augment sample tumor cell abundance should be explored, including the extraction of DNA directly from rapid onsite evaluation slides, a technique we are currently exploring. ■

**Author disclosures** are available with the text of this letter at [www.atsjournals.org](http://www.atsjournals.org).

David Fielding, M.B. B.S., F.R.A.C.P., M.D.  
The Royal Brisbane & Women's Hospital  
Herston, Brisbane, Queensland, Australia

Andrew J. Dalley, Ph.D.  
The University of Queensland Centre for Clinical Research  
Herston, Brisbane, Queensland, Australia

Farzad Bashirzadeh, M.D., F.R.A.C.P.  
Mahendra Singh, F.R.C.P.A.  
Lakshmy Nandakumar, F.R.C.P.A.  
Pathology Queensland at The Royal Brisbane & Women's Hospital  
Herston, Brisbane, Queensland, Australia

Amy E. McCart Reed, Ph.D.  
Debra Black, B.Sc. Hons.  
The University of Queensland Centre for Clinical Research  
Herston, Brisbane, Queensland, Australia

Stephen Kazakoff, Ph.D.  
Katia Nones, Ph.D.  
John Pearson, B.Sc. Hons.  
Nic Waddell, Ph.D.  
Queensland Institute of Medical Research Berghofer Medical Research  
Institute  
Herston, Brisbane, Queensland, Australia

Sunil R. Lakhani  
Pathology Queensland at The Royal Brisbane & Women's Hospital  
Herston, Brisbane, Queensland, Australia  
The University of Queensland Centre for Clinical Research  
Herston, Brisbane, Queensland, Australia  
and  
The University of Queensland School of Medicine  
Herston, Brisbane, Queensland, Australia

Peter T. Simpson, Ph.D.  
The University of Queensland Centre for Clinical Research  
Herston, Brisbane, Queensland, Australia  
and  
The University of Queensland School of Medicine  
Herston, Brisbane, Queensland, Australia

ORCID IDs: 0000-0003-2311-4919 (D.F.); 0000-0002-8362-6492 (A.J.D.); 0000-0001-5387-2791 (A.E.M.R.); 0000-0003-1925-5196 (K.N.); 0000-0003-1879-2555 (S.R.L.); 0000-0002-4816-8289 (P.T.S.).

## References

- Warren WA, Hagaman JT. Endobronchial ultrasound-guided transbronchial needle aspiration for mediastinal staging in a community medical center. *Ann Am Thorac Soc* 2016;13:1802–1807.
- Cameron SEH, Andrade RS, Pambuccian SE. Endobronchial ultrasound-guided transbronchial needle aspiration cytology: a state of the art review. *Cytopathology* 2010;21:6–26.
- Wahidi MM, Herth F, Yasufuku K, Shepherd RW, Yarmus L, Chawla M, Lamb C, Casey KR, Patel S, Silvestri GA, et al. Technical aspects of endobronchial ultrasound-guided transbronchial needle aspiration: CHEST Guideline and Expert Panel Report. *Chest* 2016;149:816–835.
- Nakajima T, Yasufuku K. How I do it: optimal methodology for multidirectional analysis of endobronchial ultrasound-guided transbronchial needle aspiration samples. *J Thorac Oncol* 2011;6:203–206.
- Wong SQ, Fellowes A, Doig K, Ellul J, Bosma TJ, Irwin D, Vedururu R, Tan AY, Weiss J, Chan KS, et al. Assessing the clinical value of targeted massively parallel sequencing in a longitudinal, prospective population-based study of cancer patients. *Br J Cancer* 2015;112:1411–1420.
- Fielding D, Bashirzadeh F, Singh M, Nandakumar L, McCart Reed A, Black D, Dalley A, Pearson J, Nones K, Waddell N, et al. Next generation sequencing on endobronchial ultrasound transbronchial needle aspirate lymph node specimens in lung cancer patients shows a high incidence of mutations and consistency with single gene testing. *Respirology* 2017;22(Suppl 2):18–100.
- Liu P, Morrison C, Wang L, Xiong D, Vedell P, Cui P, Hua X, Ding F, Lu Y, James M, et al. Identification of somatic mutations in non-small cell lung carcinomas using whole-exome sequencing. *Carcinogenesis* 2012;33:1270–1276.
- Iorio F, Knijnenburg TA, Vis DJ, Bignell GR, Menden MP, Schubert M, Aben N, Gonçalves E, Barthorpe S, Lightfoot H, et al. A landscape of pharmacogenomic interactions in cancer. *Cell* 2016;166:740–754.
- Neal JW, Dahlberg SE, Wakelee HA, Aisner SC, Bowden M, Carbone DP, Ramalingam SS. Cabozantinib (C), erlotinib (E) or the combination (E+C) as second- or third-line therapy in patients with *EGFR* wild-type (wt) non-small cell lung cancer (NSCLC): A randomized phase 2 trial of the ECOG-ACRIN Cancer Research Group (E1512) [abstract]. *J Clin Oncol* 2015;33(Suppl):8003.

10. Sun Z, Wang Z, Liu X, Wang D. New development of inhibitors targeting the PI3K/AKT/mTOR pathway in personalized treatment of non-small-cell lung cancer. *Anticancer Drugs* 2015;26:1–14.
11. Yarmus L, Akulian J, Gilbert C, Feller-Kopman D, Lee HJ, Zarogoulidis P, Lechtzin N, Ali SZ, Sathiyamoorthy V. Optimizing endobronchial ultrasound for molecular analysis: how many passes are needed? *Ann Am Thorac Soc* 2013;10:636–643.

Copyright © 2017 by the American Thoracic Society

## Loss of ATM in Airway Epithelial Cells Is Associated with Susceptibility to Oxidative Stress

To the Editor:

Ataxia-telangiectasia (A-T) is characterized by chromosomal instability, immunodeficiency, cancer susceptibility, neurodegeneration, and pulmonary disease (1). One of the cardinal features of A-T is recurrent sinopulmonary infection, which is associated with the development of bronchiectasis and interstitial lung disease (2). Respiratory disease causes significant morbidity and mortality in patients with A-T, being responsible for up to 40% of deaths (3). Respiratory infections with *Streptococcus pneumoniae*, *Staphylococcus aureus*, *Pseudomonas aeruginosa*, and *Haemophilus influenzae* have been reported (4). A recent report showed that *S. pneumoniae* caused DNA damage and apoptosis in lung cells by secretion of H<sub>2</sub>O<sub>2</sub>, an agent known to cause oxidative stress (5). In this context, there is accumulating evidence that oxidative stress is associated with A-T disease, including increased sensitivity to oxidative damage, elevated levels of reactive oxygen species in A-T cells, protection against damage by antioxidants, and the observation that ataxia-telangiectasia mutated (ATM), the protein defective in A-T, is activated by oxidative stress (6–9). On the basis of these observations, the aim of this pilot study was to determine whether airway epithelial cells from patients with A-T show increased susceptibility to oxidative stress. Some of the results of these studies have been previously reported in the form of an abstract (10).

### Methods

Primary nasal epithelial cell cultures were established from three patients with A-T and three healthy controls by obtaining nasal scrapings from the inferior turbinate of each nostril, using a purpose-designed curette (ASI Rhino-Pro; Arlington Scientific, Springville, UT) and grown in bronchial epithelial growth medium (BEGM; Lonza, Basel, Switzerland). Immunofluorescence was performed as described in Reference 11, using mouse monoclonal anti-ATM (GTX70107; GeneTex, Irvine, CA), rabbit monoclonal anti-ATM S1981 (GTX61739; GeneTex), and mouse monoclonal anti- $\gamma$ H2A histone family, member X S139 (H5912; Sigma-Aldrich, St. Louis,

MI). H<sub>2</sub>O<sub>2</sub> sensitivity assays were performed by exposing cells to varying concentrations of H<sub>2</sub>O<sub>2</sub> (H1009; Sigma-Aldrich) for 30 minutes in an incubator at 37°C, 5% CO<sub>2</sub>. Real-time imaging over the course of 24 hours was then performed on the InCuCyte (Essen BioScience, Ann Arbor, MI), and cell death was visualized using NucGreen Dead 488 ReadyProbes Reagent (Thermo Fisher Scientific, Waltham, MA). *S. pneumoniae* (serotype D39) was used to infect nasal epithelial cells  $\pm$  catalase (C9322; Sigma-Aldrich) at 1 mg/ml, and percentage of epithelial cell death was determined using TUNEL assay (11684795910; Roche, Basel, Switzerland).

### Results

We confirmed the presence of ATM protein and demonstrated that it was activated (ATM phospho-S1981) after exposure to H<sub>2</sub>O<sub>2</sub> in healthy control nasal epithelial cells but not in A-T cells as expected (Figure 1A). Activated ATM was recruited to sites of DNA damage in healthy cells, as demonstrated by colocalization with  $\gamma$ H2A histone family, member X phospho-S139, a marker of DNA double strand breaks. Because ATM responds to oxidative stress, our expectation was that A-T cells would be hypersensitive to H<sub>2</sub>O<sub>2</sub>. Figure 1B shows that A-T cells demonstrate an approximately fivefold increase in sensitivity to H<sub>2</sub>O<sub>2</sub> (500  $\mu$ M) over controls, evident over a range of concentrations from 100 to 700  $\mu$ M (Figure 1C). In the context of pulmonary disease, we predicted that cells from patients with A-T would show increased sensitivity to infection with *S. pneumoniae* because of their capacity to produce H<sub>2</sub>O<sub>2</sub>. Accordingly, we infected control and A-T nasal epithelial cells with *S. pneumoniae*. A time-dependent increase in cell killing was observed in both control and A-T, but the extent of killing was significantly greater in A-T. We demonstrated that cell killing was largely a result of toxicity from H<sub>2</sub>O<sub>2</sub>, as revealed by a significant decrease in cell killing in both control and A-T when exposed to catalase at the same time as infection (Figure 1D).

### Discussion

We demonstrated here for the first time that airway epithelial cells from patients with A-T are hypersensitive to oxidative damage to DNA. We also showed that patient epithelial cells were more sensitive than controls to the damaging effects of infection with *S. pneumoniae* and revealed that this was at least partially a result of *S. pneumoniae*-produced H<sub>2</sub>O<sub>2</sub>, as it was prevented by treatment with catalase. These data support our hypothesis that oxidative damage from recurrent infection from H<sub>2</sub>O<sub>2</sub>-producing microorganisms contributes to lung disease in patients with A-T. Here we demonstrated that *S. pneumoniae* infection sensitized A-T cells to oxidative damage. It is also evident that a number of other microorganisms that infect the respiratory system are also capable of secreting products capable of causing oxidative damage, which may also contribute to lung damage. Further identification of microorganisms present in the upper respiratory tract of children with A-T and how these contribute to respiratory disease susceptibility is likely to unravel new therapeutic approaches to prevent H<sub>2</sub>O<sub>2</sub>-induced oxidative stress. Parallel studies on lung function and structure will allow for a comprehensive picture of the state and progression of each child's respiratory disease, with subsequent improvement in clinical management. The assessment of each individual patient's upper airway microbiome, susceptibility to H<sub>2</sub>O<sub>2</sub>-induced oxidative stress, and how these translate into respiratory disease will lead to the

Supported by BrAshA-T (RM2016001474), the A-T Children's Project (RM2016000563), and the National Health and Medical Research Council (GNT1020028).

Author Contributions: Conception and design: M.F.L. and P.D.S.; data analysis and interpretation: A.J.Y., E.F., M.F.L., P.D.S., C.E.W., and D.C.; experimental performance: A.J.Y.; writing: A.J.Y., M.F.L., and P.D.S.

Originally Published in Press as DOI: 10.1164/rccm.201611-2210LE on February 16, 2017